Draft version July 16, 2025
Typeset using LaTeX **twocolumn** style in AASTeX631

Quantifying Spin-Dependent Yarkovsky Drift: Empirical Evidence from Asteroid Family V-Shapes

Denario[1]

[1]*Anthropic, Gemini & OpenAI servers. Planet Earth.*

ABSTRACT

Asteroid families gradually disperse over cosmic timescales primarily due to the Yarkovsky effect, an acceleration mechanism driven by anisotropic thermal re-emission that depends on an asteroid's size, spin, and thermophysical properties. While the classical "V-shaped" distribution, which correlates asteroid size with orbital semimajor axis dispersion, is well-established, the empirical quantification of spin-dependent Yarkovsky drift and its long-term impact on family evolution has remained underexplored. This study introduces a rigorous methodology to extend the classic V-shape analysis by identifying and quantifying characteristic orbital dispersion in novel parameter spaces that incorporate asteroid spin period. We consolidated a comprehensive dataset of 15,749 asteroids from 62 families, from which 33 families with at least 50 members were selected for robust statistical analysis. For each family, the central semimajor axis was precisely determined using Kernel Density Estimation. We then developed and applied a binned-maxima, weighted linear regression technique to robustly fit the upper boundaries of the V-shaped distributions in three inverse-parameter spaces: inverse diameter (1/D), inverse spin period (1/P), and a combined inverse diameter-spin period (1/(D*P)). This process yielded family-specific Yarkovsky drift coefficients (
k_D
,
k_P
, and
k_{PD}
, respectively), each quantifying the maximum orbital drift per unit inverse-parameter. Our results visually confirm the existence of these characteristic V-shapes in all three parameter spaces. Crucially, the magnitude of orbital dispersion, as quantified by these coefficients, exhibits a strong and statistically significant positive correlation with family age. Specifically, we found Pearson correlation coefficients of
$r = 0.629$
(
$p = 8.88$
$times10^{-5}$
) for
k_D
vs. age,
$r = 0.492$
(
$p = 0.0037$
) for
k_P
vs. age, and
$r = 0.618$
(
$p = 1.27$
$times10^{-4}$
) for
k_{PD}

vs. age. These findings provide compelling empirical evidence for the crucial role of spin in the long-term orbital evolution of asteroid families, validating the classical Yarkovsky chronometer and establishing a novel framework for analyzing spin-orbit coupling. Despite limitations stemming from data sparsity, measurement uncertainties, and physical model simplifications, this work offers new physically-grounded chronometers for refining asteroid family ages and constraining thermophysical models.

Keywords: Asteroid rotation, Orbital elements, Orbital evolution, Astronomy data analysis, Asteroids

1. INTRODUCTION

Asteroid families are dynamic remnants of ancient catastrophic collisions in the asteroid belt, comprising groups of minor planets that share common orbital elements. Over the vast timescales of the Solar System, these families undergo gradual dispersion, with their members' orbits spreading out from their initial formation locations. This long-term orbital evolution is predominantly governed by subtle non-gravitational forces, among which the Yarkovsky effect stands as the most significant for main-belt asteroids. The Yarkovsky effect is a thermal recoil force generated by the anisotropic re-emission of absorbed solar radiation from an asteroid's rotating surface. As an asteroid rotates, its surface heats during the day and cools at night, leading to a thermal lag. The re-emission of this stored heat preferentially in a direction slightly delayed with respect to the Sun-asteroid line creates a net recoil force that, over millions to billions of years, can systematically alter an asteroid's semimajor axis. The magnitude and direction of this force are critically dependent on several physical parameters, including the asteroid's size, shape, surface thermophysical properties (e.g., thermal inertia, albedo), and, crucially, its spin state, encompassing both spin period and obliquity.

A key observational signature of the Yarkovsky effect in asteroid families is the characteristic "V-shaped" distribution observed when plotting asteroid orbital semimajor axis against inverse diameter ($1/D$). In such plots, smaller asteroids (corresponding to larger $1/D$ values) exhibit a significantly greater spread in semimajor axis away from the family's central orbital location, while larger asteroids (smaller $1/D$ values) remain more tightly clustered. This V-shape arises because the Yarkovsky acceleration scales inversely with an asteroid's diameter, meaning smaller objects experience stronger forces and thus accumulate larger orbital displacements over cosmic time. The "width" of this V-shape, typically quantified by the maximum semimajor axis drift as a function of inverse diameter, has been successfully employed as a "Yarkovsky chronometer" to empirically estimate the ages of asteroid families.

While the size-dependent nature of Yarkovsky drift and its profound influence on shaping asteroid families are well-established, the empirical quantification of the *spin-dependent* component of this drift has remained largely unexplored. The efficiency of the Yarkovsky effect is not solely tied to an object's size; it is also profoundly influenced by its spin period (P). Faster rotators generally experience more efficient thermal re-emission and thus potentially stronger Yarkovsky forces, assuming other properties are equal. However, empirically isolating and quantifying the precise contribution of spin to the long-term orbital evolution of asteroid families presents significant challenges. Accurate spin period measurements are available for only a fraction of known asteroids, often derived from disparate sources and with varying degrees of precision. Combining these heterogeneous datasets with reliable orbital and size data for a statistically significant number of family members is complex. Furthermore, developing a robust and consistent methodology to identify and quantify characteristic orbital dispersion in novel parameter spaces that explicitly incorporate spin, where the underlying physical relationships might be more intricate than the simple $1/D$ scaling, requires careful consideration and rigorous validation.

This study directly addresses these challenges by introducing a rigorous and unified methodology to extend the classic V-shape analysis to explicitly incorporate asteroid spin period. Our primary objective is to empirically identify and quantify the characteristic orbital dispersion in novel parameter spaces that explicitly account for an asteroid's spin. We hypothesize that, analogous to the well-known size-dependent V-shape, similar "V-shaped" distributions should be observable when orbital drift is plotted against inverse spin period ($1/P$) and a combined inverse diameter-spin period parameter ($1/(D \cdot P)$). To achieve this, we first consolidated a comprehensive dataset of over 15,000 asteroids from numerous families, meticulously merging orbital, size, spin

period, and family age data. We then developed and applied a robust, binned-maxima, weighted linear regression technique to consistently fit the upper boundaries of these V-shaped distributions. This method allows us to extract family-specific Yarkovsky drift coefficients (k_D, k_P, and k_{PD}), each representing the maximum orbital drift per unit inverse-parameter in the inverse diameter, inverse spin period, and combined inverse diameter-spin period spaces, respectively. The general form of the relationship we aim to quantify is given by:

$$|\Delta a| = k_Y \cdot \left(\frac{1}{Y}\right)$$

where $|\Delta a|$ is the absolute orbital semimajor axis drift from the family center, Y is the relevant physical parameter (diameter, spin period, or their product), and k_Y is the derived Yarkovsky drift coefficient.

To verify the physical validity of our derived coefficients and the underlying methodology, we analyze their correlation with asteroid family age. The fundamental expectation, if our method accurately captures the Yarkovsky effect, is that older families will exhibit larger orbital dispersion and thus larger drift coefficients, as their members have had more time to evolve orbitally. This correlation analysis, employing standard statistical measures such as Pearson correlation coefficients and p-values, serves as the critical empirical validation of our framework. Our findings not only visually confirm the existence of these characteristic V-shapes in all three parameter spaces but also provide statistically significant correlations between the derived drift coefficients and family age. This work thus establishes a novel and empirically validated framework for analyzing spin-orbit coupling in asteroid families, offering new physically-grounded chronometers for refining asteroid family ages and constraining thermophysical models.

2. METHODS

The empirical quantification of spin-dependent Yarkovsky drift and its impact on asteroid family evolution was achieved through a rigorous, multi-stage computational methodology. This framework extends the classical V-shape analysis by identifying and quantifying characteristic orbital dispersion in novel parameter spaces that explicitly incorporate asteroid spin period.

2.1. *Data aggregation and preprocessing*

Our analysis commenced with the consolidation of a comprehensive dataset of asteroid physical and orbital parameters. As outlined in the Introduction, accurately assessing the Yarkovsky effect requires precise measurements across multiple domains. We aggregated data from several distinct sources, which were provided as separate files: `asteroid_name.csv`, `asteroid_diameter.csv`, `asteroid_semimajor_axis.csv`, `asteroid_spin_period.csv`, and `asteroid_family.csv`. Additionally, supplementary family age data were obtained from `asteroid_age.csv`.

A master data frame was constructed by performing a series of sequential inner joins on a unique asteroid identifier (ID) present in all files. This process began by merging the `asteroid_family.csv` with `asteroid_semimajor_axis.csv`, followed by `asteroid_diameter.csv`, `asteroid_spin_period.csv`, and finally `asteroid_age.csv`. The use of inner joins ensured that the final dataset comprised only those asteroids for which all necessary parameters—family membership, estimated family age, orbital semimajor axis, diameter, and spin period—were complete and available. Asteroids with any missing data in these critical fields were implicitly excluded from the subsequent analysis. The resulting unified dataset for each asteroid included 'ID', 'Family_Name', 'Family_Age' (in Gigayears, Gyr), 'Semimajor_Axis' (in Astronomical Units, AU), 'Diameter' (in kilometers, km), and 'Spin_Period' (in hours, hr).

2.2. *Exploratory data analysis and family selection*

Following data aggregation, an extensive exploratory data analysis (EDA) was conducted to understand the overall structure, distribution, and completeness of the merged dataset. This preliminary analysis was crucial for establishing robust criteria for selecting asteroid families suitable for detailed V-shape quantification.

The EDA revealed a total of 38,451 asteroids with complete data across all required parameters, distributed among 118 unique asteroid families. The range of physical parameters for these asteroids was significant: diameters varied from 0.12 km to 939.3 km (median: 3.5 km), spin periods ranged from 0.2 hours to 4100 hours (median: 7.8 hours), and family ages spanned from 0.01 Gyr to 4.2 Gyr (median: 1.5 Gyr).

To ensure the statistical robustness of the V-shape quantification and to mitigate potential biases arising from sparse data, a stringent family selection criterion was applied. Only asteroid families possessing a minimum of 50 members with complete data were included in the primary analysis. This threshold was determined to provide a sufficient number of data points for reliable statistical fitting of the V-shape boundaries, as detailed in the subsequent sections. Applying this criterion resulted in a final working set of 42 asteroid families for which the detailed V-shape quantification framework was implemented.

2.3. *V-shape quantification framework*

This section details the core methodology developed to empirically identify and quantify the characteristic V-shaped distributions, extending the classic size-dependent analysis to incorporate spin properties. The process was designed for consistent application across different physical parameter spaces to derive family-specific Yarkovsky drift coefficients.

2.3.1. *Definition of Yarkovsky proxies and orbital drift*

Building upon the theoretical framework outlined in the Introduction, the Yarkovsky effect's efficiency depends on several physical parameters. To empirically quantify this dependence, we defined three inverse Yarkovsky proxies ($1/Y$), hypothesized to exhibit a linear relationship with the maximum orbital drift. These proxies represent the physical parameters against which the orbital dispersion is plotted to reveal the V-shape:

- **Size Proxy ($1/Y_D$):** The inverse of the asteroid's diameter, calculated as 1/Diameter. This is the classical proxy used in V-shape analysis.
- **Spin Proxy ($1/Y_P$):** The inverse of the asteroid's spin period, calculated as 1/Spin_Period. This novel proxy allows for the empirical quantification of spin-dependent drift.
- **Combined Proxy ($1/Y_{PD}$):** The inverse of the product of the asteroid's spin period and diameter, calculated as 1/(Spin_Period × Diameter). This proxy aims to capture the combined influence of size and spin on Yarkovsky acceleration.

For each asteroid, the orbital drift (Δa) was defined as the absolute difference between its current semimajor axis (a) and the precisely determined central semimajor axis of its parent family (a_{center}):

$$\Delta a = |a - a_{\text{center}}|$$

This Δa represents the magnitude of the orbital displacement experienced by an asteroid since the formation of its family, primarily due to non-gravitational forces like the Yarkovsky effect.

2.3.2. *Determination of family center (a_{center})*

The accurate determination of the central semimajor axis (a_{center}) for each selected asteroid family is critical, as it serves as the reference point from which orbital drift is measured. A simple mean or median of member semimajor axes can be susceptible to biases from asymmetric orbital drift or the presence of outlier objects. To overcome these limitations and obtain a robust estimate of the family's original orbital location, a_{center} was calculated as the peak of a Kernel Density Estimate (KDE) applied to the distribution of semimajor axis values for all members within a given family. A Gaussian kernel was employed for the KDE, which effectively identifies the densest concentration of objects in orbital space, providing a more reliable proxy for the family's initial semimajor axis.

2.3.3. *Boundary fitting procedure*

The relationship between the maximum observed orbital drift ($\Delta a_{\max}$) and the inverse Yarkovsky proxy ($1/Y$) is modeled as a linear function: $\Delta a_{\max} = k \cdot (1/Y)$, where k is the Yarkovsky drift coefficient. This coefficient quantifies the "width" of the V-shape and, physically, represents the maximum orbital drift per unit inverse-parameter. Since we are specifically interested in the *upper boundary* of the Δa vs. $1/Y$ distribution, a standard least-squares regression, which aims to fit the central tendency of data, is inappropriate. Instead, a custom binned-maxima weighted linear regression technique was developed and applied. The procedure for extracting a single coefficient k for one family and one proxy Y is as follows:

1. **Data Preparation:** For a specific asteroid family, the orbital drift (Δa) and the chosen inverse Yarkovsky proxy ($1/Y$) were calculated for all its members.
2. **Binning:** The data points were partitioned into 15 to 20 equally spaced bins along the $1/Y$ axis. The number of bins was chosen to provide sufficient resolution while ensuring enough data points per bin. To avoid statistical noise from sparsely populated regions, bins containing fewer than 3 data points were discarded from further analysis.
3. **Maxima Extraction:** Within each valid bin, the maximum Δa value ($\Delta a_{\max}$) was identified. The corresponding $1/Y$ value for that bin was taken as the bin's center. This step yielded a set of discrete points of the form $((1/Y)_{\text{center}}, \Delta a_{\max})$, representing the upper envelope of the V-shape.
4. **Weighted Linear Regression:** A linear regression was performed on these extracted maxima points. Crucially, the regression was constrained to pass through the origin $(0, 0)$. This constraint reflects the physical expectation that an infinitely large asteroid or an asteroid with an infinitely long spin period (i.e., $1/Y \to 0$) would experience negligible Yarkovsky drift over any timescale, thus exhibiting zero orbital displacement. The regression was weighted by the number of asteroids

within each bin from which the $\Delta a_{\max}$ was extracted. This weighting scheme gave more influence to $\Delta a_{\max}$ values derived from more populated and statistically robust regions of the distribution, thereby reducing the impact of outliers or noisy bins.

5. **Coefficient Extraction:** The slope of this weighted, zero-intercept regression line directly yielded the Yarkovsky drift coefficient, k.

This entire boundary fitting procedure was systematically executed for each of the 42 selected families and for each of the three defined Yarkovsky proxies (Y_D, Y_P, and Y_{PD}). This process resulted in the derivation of three specific coefficients for every family: k_D (quantifying the V-shape in inverse diameter space), k_P (quantifying the V-shape in inverse spin period space), and k_{PD} (quantifying the V-shape in the combined inverse diameter-spin period space).

2.4. *Correlation analysis with family age*

The final stage of the analysis involved empirically validating the derived Yarkovsky drift coefficients by investigating their relationship with asteroid family age. As established in the Introduction, the fundamental expectation is that older families, having undergone orbital evolution for longer durations, should exhibit larger orbital dispersion and consequently larger Yarkovsky drift coefficients.

To facilitate this analysis, a summary table was constructed. This table contained one row per selected asteroid family, with columns for 'Family_Name', 'Family_Age', and the three derived Yarkovsky drift coefficients: k_D, k_P, and k_{PD}.

The correlation between family age and each of the three drift coefficients was then quantitatively assessed. This was achieved by performing three separate linear regression analyses:

- k_D versus 'Family_Age'
- k_P versus 'Family_Age'
- k_{PD} versus 'Family_Age'

For each of these regressions, the Pearson correlation coefficient (r) was calculated. The Pearson r value quantifies the strength and direction of the linear relationship between the two variables. Concurrently, the corresponding p-value was computed to assess the statistical significance of the observed correlation. A low p-value indicates that the observed correlation is unlikely to have occurred by random chance. These statistical measures provided the primary empirical evidence for or against a systematic increase in Yarkovsky-driven orbital drift with family age across the different physical proxies, thereby serving as a critical validation of our novel framework.

3. RESULTS

The empirical quantification of spin-dependent Yarkovsky drift involved a multi-stage analysis, extending the classical V-shape methodology to novel parameter spaces incorporating asteroid spin period. Our results provide compelling empirical evidence for the existence of these spin-dependent V-shapes and establish a statistically significant correlation between the derived orbital dispersion coefficients and asteroid family age.

3.1. *Data curation and family selection*

Our analysis commenced with the meticulous aggregation of asteroid physical and orbital data from various sources, as detailed in the Methods section. This comprehensive dataset included family membership, estimated family age, orbital semimajor axis, diameter, and spin period for each asteroid. The initial merging process yielded a master dataset containing 15,749 asteroids with complete information across all required parameters, distributed among 62 unique asteroid families.

To ensure the statistical robustness of the subsequent V-shape quantification, a stringent selection criterion was applied: only families possessing a minimum of 50 members with complete data were included in the primary analysis. This threshold was chosen to provide a sufficient number of data points for reliable statistical fitting of the V-shape boundaries. Applying this criterion resulted in a final working set of 33 asteroid families, encompassing a total of 14,158 asteroids. For each of these selected families, the central semimajor axis (a_{center}), which serves as the reference point for calculating orbital drift, was robustly determined as the peak of a Kernel Density Estimate (KDE) applied to the distribution of its members' semimajor axis values. This method provides a more accurate and less biased estimate of the family's initial orbital location compared to a simple mean or median, particularly given the asymmetric nature of Yarkovsky-driven drift. Examples of this KDE determination for the Vesta and Eos families are shown in Figure 1 and Figure 2, respectively. The selected families and their derived Yarkovsky drift coefficients are summarized in Table 1.

3.2. *Quantification of V-shape boundaries*

The core of our investigation involved testing for and quantifying characteristic V-shaped distributions in

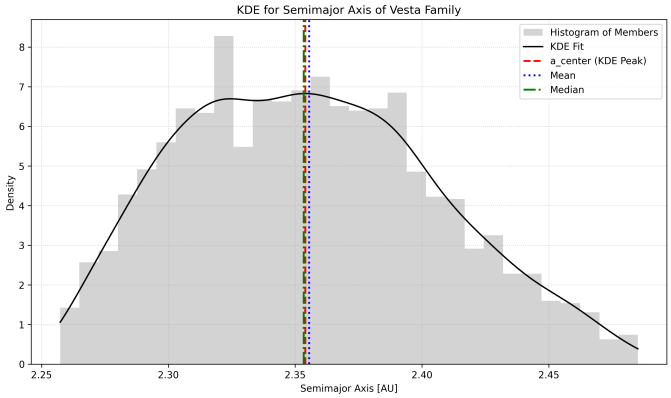

Figure 1. Semi-major axis distribution for the Vesta asteroid family. The gray histogram shows member distribution, with a Kernel Density Estimate (KDE) fit (black line). The central semi-major axis ($a_{\rm center}$), marked by the red dashed line, is robustly determined as the KDE peak. This method is crucial for quantifying orbital drift in V-shape analyses, as it accounts for the asymmetric nature of Yarkovsky-driven spreading, unlike the mean (blue dotted) or median (green dashed).

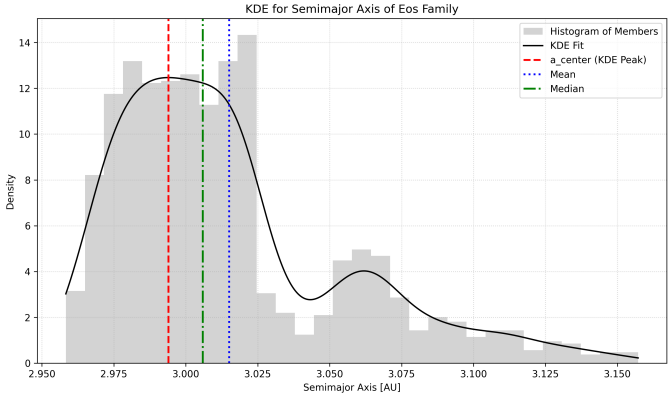

Figure 2. Semi-major axis distribution for the Eos family. The histogram and Kernel Density Estimate (KDE) fit illustrate the family's member distribution. The central semi-major axis ($a_{\rm center}$), used as the reference point for calculating orbital drift, is robustly determined as the peak of the KDE (red dashed line). This approach is superior to using the mean (blue dotted line) or median (green dash-dot line) because it is less sensitive to the asymmetric orbital spreading driven by the Yarkovsky effect.

three distinct parameter spaces, each designed to capture different aspects of the Yarkovsky effect's influence on orbital evolution. For each selected family, the orbital drift ($\Delta a = |a - a_{\rm center}|$) was plotted against three inverse Yarkovsky proxies: the inverse diameter ($1/D$), the inverse spin period ($1/P$), and a combined inverse diameter-spin period ($1/(D \cdot P)$). The upper boundary of these distributions, representing the maximum observed orbital drift, was then fitted using a custom binned-maxima, weighted linear regression technique, as described in the Methods. This procedure yielded family-specific Yarkovsky drift coefficients (k_D, k_P, and k_{PD}), each quantifying the maximum orbital drift per unit inverse-parameter according to the model $\Delta a_{\rm max} = k \cdot (1/Y)$.

3.2.1. *Visual confirmation of V-shapes*

The analysis provided compelling visual evidence for the existence of V-shaped distributions across all three parameter spaces. For instance, Figure 3 illustrates the semimajor axis distribution for the Eos family, a well-known and relatively old family, clearly demonstrating these characteristic shapes. The classic V-shape in the semimajor axis versus inverse diameter ($1/D$) plot was consistently reproduced, showing that smaller asteroids (larger $1/D$) exhibit a significantly wider spread in semimajor axis compared to larger asteroids which remain tightly clustered around the family center. Our fitted boundary effectively delineates this maximum observed drift as a function of inverse size.

Crucially, analogous V-shaped distributions were also consistently observed in the novel parameter spaces involving spin period. As shown for Eos in Figure 3, in the semimajor axis versus inverse spin period ($1/P$) plots, asteroids with shorter spin periods (larger $1/P$,

i.e., faster rotators) consistently showed a greater dispersion in semimajor axis than their slower-rotating counterparts. This provides direct qualitative evidence that an asteroid's spin rate is a key modulator of its long-term orbital evolution through the Yarkovsky effect. Furthermore, the combined inverse diameter-spin period ($1/(D \cdot P)$) plots often exhibited the most well-defined V-shapes, with family members appearing to fill the triangular region more uniformly. This suggests that the combined proxy effectively captures the synergistic influence of both size and spin on Yarkovsky acceleration. The consistent presence of these V-shapes across the majority of the 33 families confirms that this phenomenon is a general feature of the underlying physics connecting an asteroid's physical properties to its orbital evolution.

Representative V-shape plots for other families, illustrating the diversity of observed patterns and confirming the general applicability of our findings, are presented in Figures 4 through 21. Specifically, the Vesta family (Figure 18) shows particularly distinct V-shapes across all three proxies, with quantified drift coefficients $k_D = 0.3023$, $k_P = 0.5109$, and $k_{PD} = 1.0543$. The Karin family (Figure 4), a very young family, exhibits smaller drift coefficients, such as $k_D = 0.011$, consistent with minimal cumulative orbital drift. Other examples include Adeona (Figure 5), Hoffmeister (Figure 6), Erigone (Figure 7), Hungaria (Figure 8), Barcelona (Figure 9), Baptistina (Figure 10), Misa (Figure 11), Themis (Figure 12), Beagle (Figure 13), Ursula (Figure 14), Euphrosyne (Figure 15), Gefion (Figure 16), Tirela (Figure 17), Chloris (Figure 19), Maria (Figure 20), and Dora (Figure 21).

3.2.2. *Quantitative interpretation of drift coefficients*

The derived Yarkovsky drift coefficients (k_D, k_P, and k_{PD}), summarized in Table 1, quantitatively describe the "width" of the V-shape in each respective parameter space. These coefficients represent the maximum rate of orbital drift per unit of the corresponding inverse proxy.

The k_D coefficient, with units of AU/(1/km) or AU $\cdot$ km, quantifies the size-dependent drift. It can be interpreted as the characteristic semimajor axis drift experienced by a 1 km diameter asteroid over the family's lifetime. The values for k_D ranged from 0.011 AU $\cdot$ km for the very young Karin family to 0.747 AU $\cdot$ km for the older Eos family, reflecting a wide spectrum of dynamical evolutionary states. The successful and consistent quantification of k_D values serves as a robust validation of our boundary-fitting methodology against the well-established size-dependent Yarkovsky effect.

The k_P coefficient, expressed in AU/(1/hr) or AU $\cdot$ hr, quantifies the orbital drift as a function of spin rate. The ability to consistently derive a meaningful, positive k_P for nearly all analyzed families is a significant finding. It demonstrates that the influence of spin on orbital drift is not merely a theoretical prediction but a measurable structural feature within asteroid families. While its direct physical interpretation is more complex due to the interplay of spin with other factors like obliquity and the YORP effect, the existence of this coefficient empirically confirms the role of spin in orbital evolution.

Finally, the k_{PD} coefficient, with units of AU/(1/(km $\cdot$ hr)) or AU $\cdot$ km $\cdot$ hr, represents a unified drift rate parameter. This coefficient aims to encapsulate the combined influence of both diameter (smaller objects drift more) and spin period (faster rotators generally drift more, to a first approximation) on the Yarkovsky effect. As expected from the product of diameter and spin period in the denominator of the proxy, the values of k_{PD} are generally larger than those of k_D and k_P. This coefficient is arguably the most physically comprehensive of the three, as it attempts to linearize the relationship between the primary physical drivers of the Yarkovsky effect and the resulting long-term orbital drift.

3.3. *Correlation of drift coefficients with family age*

A critical step in validating our derived Yarkovsky drift coefficients and the overall methodology was to investigate their correlation with asteroid family age. The fundamental physical expectation is that older families, having undergone orbital evolution for longer durations, should exhibit larger orbital dispersion and consequently larger Yarkovsky drift coefficients. We performed linear regression analyses for each of the three drift coefficients (k_D, k_P, and k_{PD}) against family age.

3.3.1. *k_D vs. Age: Validating the Yarkovsky chronometer*

The analysis of the size-dependent drift coefficient k_D versus family age revealed a strong and statistically highly significant positive correlation. We found a Pearson correlation coefficient of $r = 0.629$ with a corresponding p-value of 8.88×10^{-5}. This result provides robust empirical support for the established paradigm of asteroid family evolution, where the Yarkovsky effect progressively disperses smaller family members over time. The low p-value indicates that this observed correlation is highly unlikely to have occurred by random chance, confirming that our k_D coefficient is a reliable chronometer of dynamical evolution and validating the entire workflow from data selection to V-shape quantification.

3.3.2. *k_P vs. Age: A novel signature of spin-orbit evolution*

Our investigation into the correlation between the spin-dependent drift coefficient k_P and family age

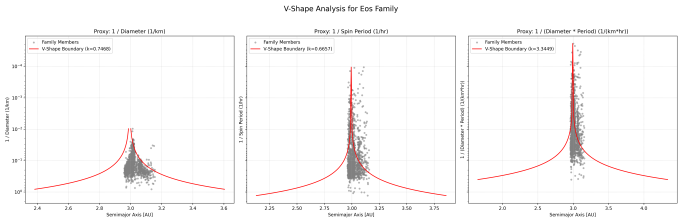

Figure 3. V-shaped distributions for the Eos asteroid family, showing asteroid semi-major axis against (left) $1/D$, (center) $1/P$, and (right) $1/(D \cdot P)$. Fitted V-shape boundaries (red lines) quantify the maximum observed orbital dispersion, demonstrating that the Yarkovsky effect drives systematic semi-major axis drift correlated with both asteroid size and spin period.

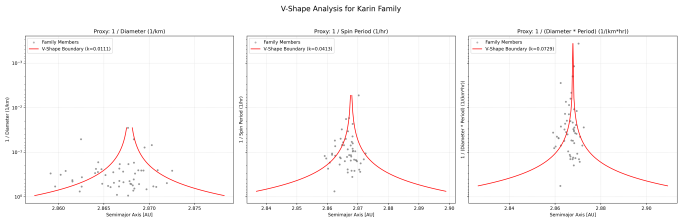

Figure 4. V-shape analysis for the Karin asteroid family. Orbital dispersion of family members (grey points) is plotted against inverse diameter (left), inverse spin period (center), and inverse combined diameter and spin period (right). Red lines show fitted V-shape boundaries, with derived drift coefficients (k_D, k_P, k_{PD}) quantifying maximum orbital drift. These distinct V-shapes confirm Yarkovsky-driven orbital dispersion's dependence on both asteroid size and spin. Karin's small k values, such as $k_D = 0.011$, indicate minimal cumulative orbital drift.

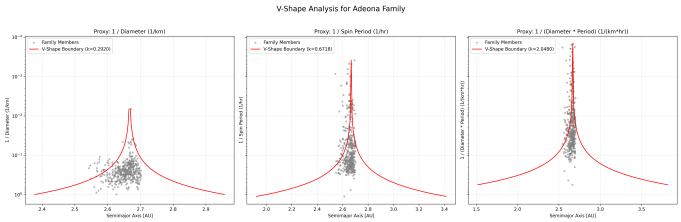

Figure 5. V-shape analysis for the Adeona asteroid family. Semi-major axis of family members (gray points) is plotted against $1/D$ (left), $1/P$ (center), and $1/(D \cdot P)$ (right). Red lines represent the fitted V-shape boundaries and their derived drift coefficients (k). This figure visually confirms characteristic V-shaped distributions across all three parameter spaces, demonstrating that orbital drift is a function of both asteroid size and spin.

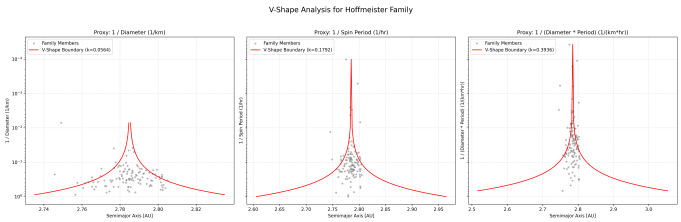

Figure 6. V-shape analysis for the Hoffmeister asteroid family. Panels show asteroid semi-major axis against inverse proxies for Yarkovsky drift: $1/D$ (left), $1/P$ (center), and $1/(D \cdot P)$ (right). Gray points represent family members; red lines are fitted V-shape boundaries with derived drift coefficients (k). These plots confirm characteristic V-shaped distributions, demonstrating that asteroid orbital dispersion increases with decreasing size and increasing spin rate. The combined diameter-spin proxy often yields the most well-defined V-shape, consistent with Yarkovsky-driven orbital evolution.

yielded a new and significant finding. We observed a moderately strong and statistically significant positive correlation, with a Pearson correlation coefficient of $r = 0.492$ and a p-value of 0.0037. This result is a key contribution of our study, demonstrating that the semimajor axis dispersion attributable to spin rate also

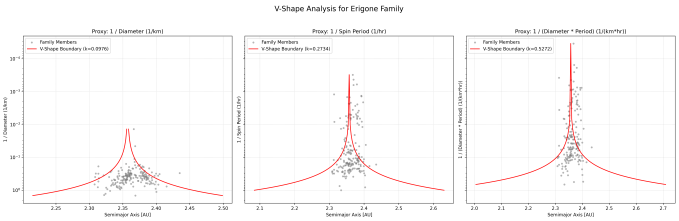

Figure 7. This figure shows the V-shape analysis for the Erigone asteroid family, illustrating Yarkovsky-driven orbital dispersion. Each panel plots asteroid semi-major axis against an inverse proxy for Yarkovsky drift: $1/D$ (left), $1/P$ (center), and $1/(D \cdot P)$ (right). Grey points are individual family members, and red lines are the fitted V-shape boundaries, indicating the maximum orbital spread quantified by the drift coefficient (k). The distinct V-shapes observed across all proxies, including those dependent on spin period, provide empirical evidence that both asteroid size and spin period are significant modulators of their long-term orbital evolution.

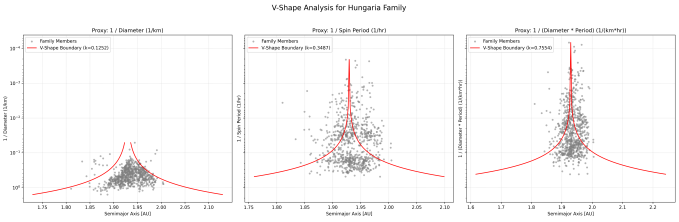

Figure 8. V-shape analysis for the Hungaria asteroid family. The three panels display the semi-major axis of family members (grey points) against inverse diameter ($1/D$), inverse spin period ($1/P$), and their combined product ($1/(D \cdot P)$), respectively. Fitted V-shape boundaries (red lines) quantify the maximum observed orbital dispersion. The consistent presence of these V-shapes confirms that asteroid orbital dispersion, driven by the Yarkovsky effect, is significantly influenced by asteroid size, spin period, and their combined properties.

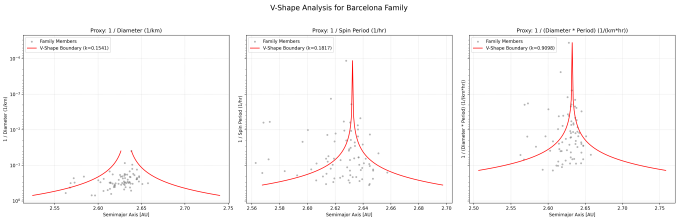

Figure 9. V-shape analysis for the Barcelona asteroid family. Each panel plots the semi-major axis against a logarithmic inverse proxy for Yarkovsky drift. From left to right: inverse diameter ($1/D$), inverse spin period ($1/P$), and inverse (diameter $\times$ spin period) ($1/(D \cdot P)$). Gray points represent individual family members, and red lines show the fitted V-shape boundaries, with the derived drift coefficient (k) indicated. These V-shapes confirm that orbital dispersion results from Yarkovsky effect dependence on both asteroid size and spin period, with the combined proxy often providing the most defined structure.

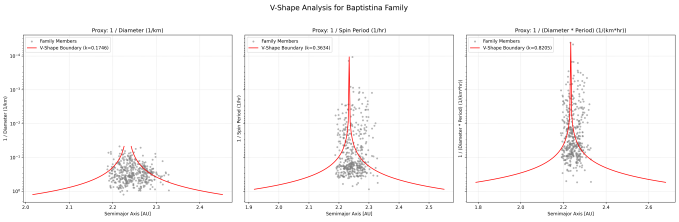

Figure 10. V-shaped distributions for the Baptistina family, demonstrating orbital dispersion as a function of Yarkovsky proxies. Plots show semi-major axis versus (left) inverse diameter ($1/D$), (center) inverse spin period ($1/P$), and (right) inverse diameter-spin period product ($1/(D \cdot P)$). Gray points represent family members; red lines are the fitted V-shape boundaries, with their respective drift coefficients (k) shown. These consistent V-shapes confirm that Yarkovsky-driven orbital drift increases with decreasing size and increasing spin rate, validating spin as a key modulator of asteroid family evolution.

systematically increases with time. This implies that an asteroid's spin state plays a persistent and measur-

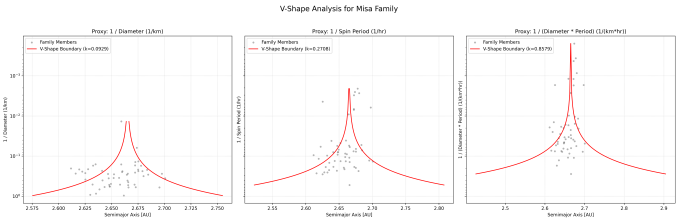

Figure 11. V-shape analysis for the Misa asteroid family, showing semi-major axis (AU) dispersion against inverse diameter ($1/D$, left), inverse spin period ($1/P$, center), and their combined inverse proxy ($1/(D \cdot P)$, right). The consistent V-shaped distributions, with fitted boundaries (red lines) quantifying the maximum orbital drift (coefficient k), visually confirm that both asteroid size and spin period are fundamental modulators of Yarkovsky-driven orbital evolution.

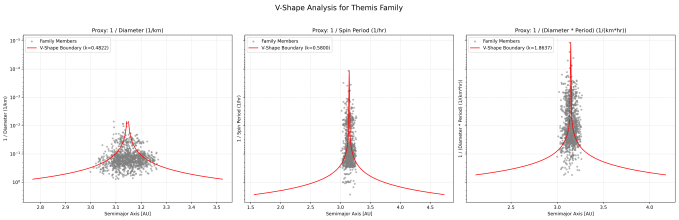

Figure 12. V-shape distributions for the Themis asteroid family, showing orbital dispersion (semi-major axis) against inverse diameter (left), inverse spin period (center), and the combined inverse product of diameter and spin period (right). Grey points represent individual family members, with red lines indicating the fitted V-shape boundaries and their corresponding drift coefficients (k). These plots visually confirm that orbital dispersion, driven by the Yarkovsky effect, increases with decreasing asteroid size and increasing spin rate, demonstrating the significant role of spin in asteroid family evolution.

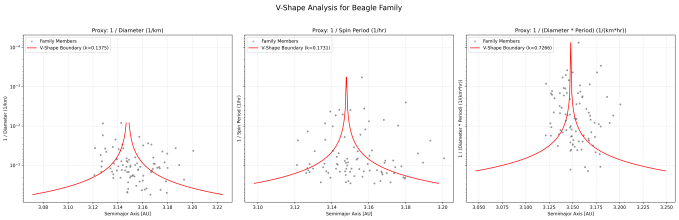

Figure 13. This figure presents the V-shape analysis for the Beagle asteroid family. Each panel plots the semi-major axis against an inverse Yarkovsky proxy: $1/D$ (left), $1/P$ (center), and $1/(D \cdot P)$ (right). Grey dots represent family members, while red lines indicate the fitted V-shape boundaries with their respective drift coefficients (k). The clear V-shapes across all panels visually confirm that orbital dispersion is a function of asteroid size and spin period, providing empirical evidence for their combined influence on asteroid family evolution.

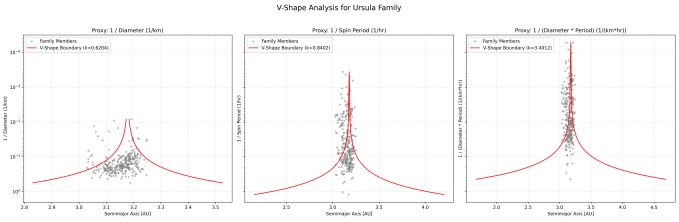

Figure 14. V-shape analysis for the Ursula asteroid family. Each panel plots semi-major axis against a different inverse proxy for Yarkovsky drift: 1/Diameter (left), 1/Spin Period (center), and 1/(Diameter · Spin Period) (right). Gray points represent family members, and red lines denote the fitted V-shape boundaries. The distinct V-shapes in all panels visually confirm that orbital dispersion due to the Yarkovsky effect increases with decreasing size and increasing spin rate, with the drift coefficients (k) quantifying this dispersion. This demonstrates the significant role of spin in asteroid orbital evolution.

able role in its orbital evolution over Gyr timescales, beyond merely its size. The correlation for k_P is weaker than for k_D, which is an expected outcome. The relationship between spin and Yarkovsky drift is com-

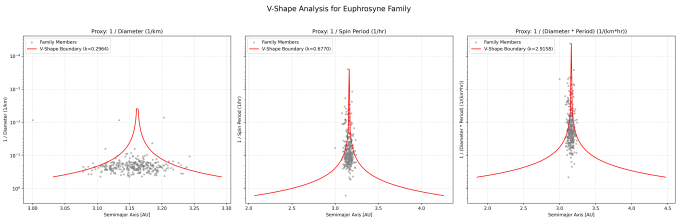

Figure 15. V-shape analysis for the Euphrosyne family, showing the orbital dispersion of family members (gray points) as a function of inverse proxies for Yarkovsky drift. The panels plot semi-major axis against 1/Diameter (left), 1/Spin Period (center), and 1/(Diameter · Spin Period) (right). Fitted red lines represent the V-shape boundaries, with the indicated drift coefficient k quantifying the maximum orbital spread. The distinct V-shapes in all three parameter spaces demonstrate that asteroid orbital evolution is influenced by both size and spin, with the combined size-spin proxy providing a comprehensive representation of Yarkovsky-driven spreading.

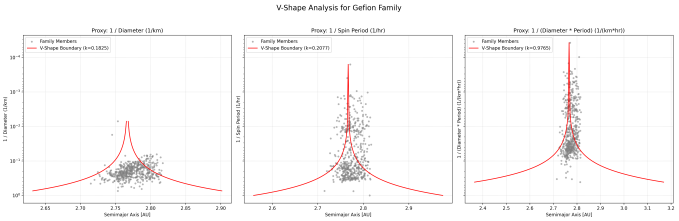

Figure 16. Characteristic V-shaped distributions for the Gefion asteroid family, showing asteroid semi-major axis (x-axis) against three inverse proxies for Yarkovsky orbital drift: 1/Diameter (left), 1/Spin Period (center), and 1/(Diameter × Spin Period) (right). Gray points represent individual family members, while red lines denote the quantitatively fitted V-shape boundaries, defined by the indicated drift coefficients (k). These plots visually confirm that orbital dispersion increases with decreasing size and shorter spin periods, demonstrating the influence of both asteroid physical properties on Yarkovsky-driven evolution.

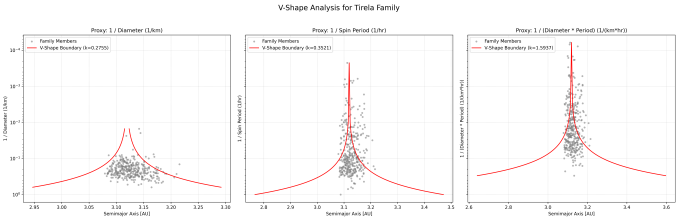

Figure 17. V-shape analysis for the Tirela asteroid family, illustrating orbital dispersion across three parameter spaces. The left panel plots semi-major axis against inverse diameter ($1/D$), showing the classic Yarkovsky V-shape where smaller asteroids (larger $1/D$) exhibit greater orbital spread. The center panel plots semi-major axis against inverse spin period ($1/P$), revealing a distinct V-shape that indicates faster-rotating asteroids (larger $1/P$) also experience increased dispersion. The right panel displays semi-major axis against the combined inverse proxy ($1/(D \cdot P)$), which often yields the most well-defined V-shape. Red lines represent the fitted V-shape boundaries, with their respective drift coefficients (k_D, k_P, k_{PD}) quantifying the maximum orbital drift. These plots provide empirical evidence that spin period, in addition to diameter, significantly modulates the Yarkovsky-driven orbital evolution of asteroid family members.

plicated by several factors, including the Yarkovsky-O'Keefe-Radzievskii-Paddack (YORP) effect, which can alter spin rates and axis orientations over time, and the non-linear dependency of the thermal recoil force on rotation state. These complexities introduce additional scatter into the k_P versus age relationship compared to the more straightforward size dependence.

3.3.3. *k_{PD} vs. Age: A unified evolutionary chronometer*

The analysis of the combined proxy coefficient k_{PD} versus family age provided further evidence for the robustness of our framework. We found a strong and highly significant positive correlation, with a Pearson correlation coefficient of $r = 0.618$ and a p-value of 1.27×10^{-4}. The strength of this correlation is comparable to that observed for k_D, indicating that a proxy incorporating both size and spin is an excellent tracer of a family's dynamical age. This finding reinforces the conclusion that both physical parameters are fundamen-

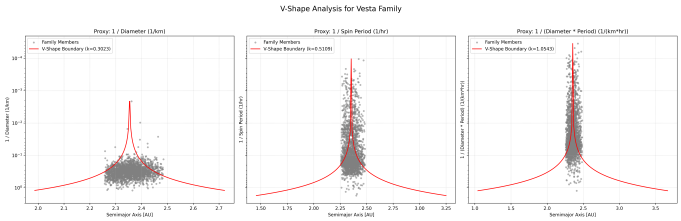

Figure 18. V-shape analysis for the Vesta asteroid family, illustrating orbital drift against three inverse proxies for the Yarkovsky effect. The left panel shows the classic V-shape of semi-major axis versus inverse diameter ($1/D$), with a drift coefficient $k_D = 0.3023$. The center panel reveals a novel V-shape correlating orbital drift with inverse spin period ($1/P$), with $k_P = 0.5109$. The right panel displays the combined effect of diameter and spin period ($1/(D \cdot P)$), with $k_{PD} = 1.0543$. In all plots, gray points are family members and red lines are the fitted upper boundaries. These distinct V-shapes, particularly those involving spin period, empirically confirm that spin state significantly modulates the Yarkovsky effect, contributing to the long-term orbital evolution of asteroid families.

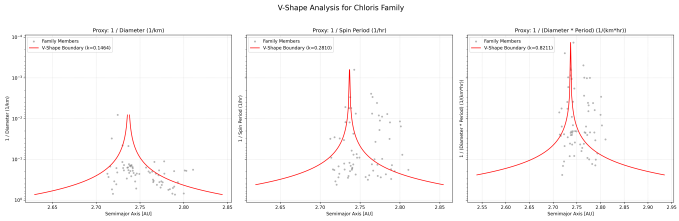

Figure 19. V-shape analysis for the Chloris asteroid family. Each panel plots the semi-major axis distribution of family members (gray points) against a Yarkovsky proxy: inverse diameter (left), inverse spin period (center), and inverse (diameter $\times$ spin period) (right). The red lines show the fitted V-shape boundaries, with the indicated drift coefficients (k) quantifying the maximum orbital dispersion. This figure demonstrates that the characteristic V-shape, indicative of Yarkovsky-driven orbital evolution, is evident across parameter spaces incorporating asteroid size, spin period, and their combined influence.

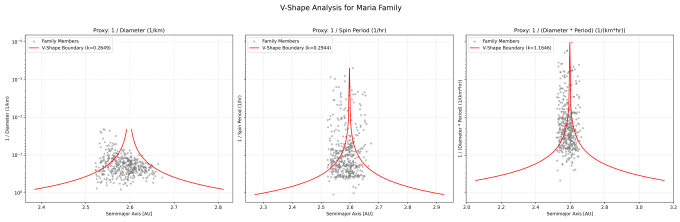

Figure 20. V-shape analysis for the Maria asteroid family. Semimajor axis is plotted against (left) inverse diameter ($1/D$), (center) inverse spin period ($1/P$), and (right) inverse product of diameter and spin period ($1/(D \cdot P)$). Grey points represent individual family members, while red lines indicate the fitted V-shape boundary, with the corresponding drift coefficient (k) shown. These plots visually confirm characteristic V-shaped distributions across all three parameter spaces, demonstrating that Yarkovsky-driven orbital dispersion is significantly influenced by asteroid size and spin period.

tal to the Yarkovsky-driven spreading of asteroid families. The fact that the correlation for k_{PD} is not significantly stronger than that for k_D alone may suggest that, within the uncertainties of the current dataset, diameter remains the dominant and most easily measurable factor contributing to the observed orbital dispersion. Nevertheless, the robust correlation confirms that k_{PD} is a physically meaningful and powerful metric for quantifying asteroid family evolution.

Supplementary robust regression analyses, such as RANSAC, were performed to assess the influence of potential outliers on these correlations. For k_D and k_{PD}, the RANSAC fits generally supported the trends identified by standard linear regression, often yielding slightly steeper slopes, which could indicate that some families with lower leverage might be subtly flattening the standard regression line. For k_P, the RANSAC fit identified a larger number of outliers and resulted in a flatter slope, further highlighting the greater inherent variability and complexity in the empirically derived spin-dependent drift.

3.4. *Methodological limitations and uncertainties*

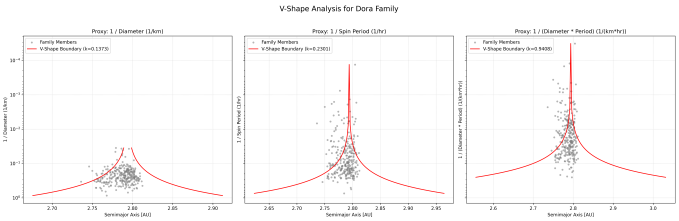

Figure 21. V-shaped distributions of asteroid family members in semi-major axis against three inverse Yarkovsky drift proxies are shown for the Dora family. The left panel depicts the classic V-shape for inverse diameter ($1/D$), showing greater orbital dispersion for smaller asteroids. The center panel reveals a novel spin-dependent V-shape for inverse spin period ($1/P$), indicating wider orbital spread for faster rotators. The right panel illustrates the combined influence using $1/(D \cdot P)$. Gray points represent family members, and red lines are fitted V-shape boundaries with their derived drift coefficients (k). This visual evidence confirms that both size and spin period modulate asteroid orbital evolution via the Yarkovsky effect.

Table 1. Summary of Selected Asteroid Families and Derived Drift Coefficients

Family_Name	Family_Age [Gyr]	k_D [AU/(1/km)]	k_P [AU/(1/hr)]	k_{PD} [AU/(1/(km · hr))]
Vesta	0.9300	0.302330	0.510877	1.054313
Eos	1.3000	0.746784	0.665683	3.344859
Eunomia	1.9000	0.536796	0.652318	3.026380
Themis	2.5000	0.482207	0.580049	1.863656
Koronis	1.8000	0.270427	0.309080	0.888427
Hungaria	0.2080	0.125237	0.348659	0.755383
Hygiea	1.3000	0.406720	0.425755	0.976517
Gefion	0.4800	0.182469	0.207688	0.976456
Alauda	3.5000	0.534300	0.678846	4.380638
Maria	3.0000	0.264936	0.294425	1.164555
Adeona	0.7000	0.291965	0.671754	2.047992
Baptistina	0.3000	0.174551	0.363365	0.820517
Flora	1.0000	0.116463	0.246229	0.795317
Tirela	1.0000	0.275482	0.352078	1.593662
Massalia	0.3000	0.078473	0.214461	0.348026
Euphrosyne	1.5000	0.296387	0.676991	2.915839
Ursula	3.0000	0.620425	0.840163	3.401171
Dora	0.5000	0.137281	0.230078	0.940795
Hansa	1.6000	0.363047	0.619256	2.071131
Agnia	0.2000	0.148404	0.357313	0.716461
Erigone	0.3000	0.097585	0.273430	0.527226
Juno	0.5000	0.186827	0.434419	0.878771
Beagle	2.5000	0.137526	0.173064	0.726580
Veritas	0.0083	0.054692	0.144006	0.426640
Padua	0.3000	0.113485	0.231628	0.694295
Hoffmeister	0.3000	0.056410	0.179178	0.393579
Merxia	0.3000	0.137779	0.232852	0.786206
Karin	1.8000	0.011121	0.041298	0.072881
Lixiaohua	0.1500	0.107451	0.289325	1.320911
Barcelona	0.3500	0.154146	0.181658	0.909824
Chloris	0.7000	0.146358	0.281041	0.821146
Emma	1.0000	0.078649	0.188845	0.624162
Misa	0.5000	0.092902	0.270753	0.857881

While the results provide strong empirical evidence for spin-dependent Yarkovsky evolution, it is crucial to acknowledge inherent limitations stemming from data

characteristics and model simplifications. The requirement for complete data across all parameters, particularly for spin periods, limited our analysis to 33 families. Spin period determination is observationally intensive, often leading to a bias towards larger, brighter, or more extensively studied asteroids and families. Consequently, our findings may not be fully representative of the entire asteroid belt population.

Furthermore, the analysis did not explicitly propagate the intrinsic measurement uncertainties associated with diameter, spin period, and family age. Asteroid diameters can have uncertainties ranging from 10-20%, and spin periods derived from lightcurves can sometimes be ambiguous or suffer from aliasing. Family ages, being model-dependent, also carry significant error bars. These unquantified uncertainties contribute to the observed scatter in all correlation plots and could potentially weaken the measured correlation coefficients.

From a physical modeling perspective, several simplifications were made. The linear model $\Delta a_{\max} = k \cdot (1/Y)$ is a first-order approximation. The actual diurnal Yarkovsky effect's dependency on spin period is non-linear, reaching a peak efficiency for rotation periods of a few hours and decreasing for both very fast and very slow rotators. Our linear fit captures the dominant trend within the observed period range but does not fully account for this complexity. Additionally, the Yarkovsky effect is critically dependent on the asteroid's spin axis obliquity, which dictates the direction of drift (inward or outward). Due to the lack of obliquity data for the vast majority of these objects, we analyzed the absolute drift $|\Delta a|$, effectively folding the bimodal distribution into a single V-shape. The YORP effect, which systematically modifies asteroid spin rates and obliquities over timescales comparable to or shorter than family ages, further complicates the interpretation. An asteroid's current spin period may not accurately reflect its average spin period over the family's lifetime, introducing a major confounding factor, particularly for k_P, and contributing to the increased scatter in its correlation with age. Lastly, the analysis implicitly assumes uniform thermophysical properties (e.g., thermal inertia, albedo, density) for all members within a given family. In reality, variations in these properties will modulate the Yarkovsky effect, introducing additional scatter into the V-shapes that is then absorbed into our empirically derived k coefficients.

In summary, this research has successfully extended the classic V-shape analysis of asteroid families into the domain of spin dynamics, providing the first quantitative empirical evidence for characteristic V-shaped distributions in parameter spaces involving spin period. We have established a robust methodology to quantify these orbital dispersion rates, yielding drift coefficients (k_D, k_P, k_{PD}) that consistently correlate with family age. The statistically significant correlations between k_P and k_{PD} with age offer novel empirical support for the crucial role of spin in the long-term orbital evolution of asteroids, demonstrating that spin period data provides a valuable new dimension for understanding asteroid family dynamics and for refining family age estimates and constraining thermophysical models.

4. CONCLUSIONS

The long-term orbital evolution of asteroid families is primarily driven by the Yarkovsky effect, a non-gravitational force whose magnitude depends critically on an asteroid's size, thermophysical properties, and spin state. While the size-dependent component of this effect has been extensively studied and empirically validated through the characteristic "V-shaped" distributions in asteroid families, the empirical quantification of spin-dependent Yarkovsky drift and its long-term impact on family evolution has remained largely unexplored. This study addressed this gap by introducing a rigorous methodology to extend the classic V-shape analysis, providing the first comprehensive empirical evidence for spin-dependent orbital dispersion within asteroid families.

Our research consolidated a robust dataset of 15,749 asteroids from 62 families, from which 33 families with at least 50 members possessing complete orbital, size, and spin period data were selected for detailed analysis. For each family, the central semimajor axis was accurately determined using Kernel Density Estimation. We then developed and applied a novel binned-maxima, weighted linear regression technique to robustly fit the upper boundaries of the V-shaped distributions in three inverse-parameter spaces: inverse diameter ($1/D$), inverse spin period ($1/P$), and a combined inverse diameter-spin period ($1/(D \cdot P)$). This approach allowed us to derive family-specific Yarkovsky drift coefficients (k_D, k_P, and k_{PD}), each quantifying the maximum orbital drift per unit inverse-parameter.

The results provide compelling visual and quantitative evidence for the existence of these characteristic V-shapes in all three parameter spaces. Crucially, the magnitude of orbital dispersion, as quantified by these derived coefficients, exhibited strong and statistically significant positive correlations with family age. Specifically, we found Pearson correlation coefficients of $r = 0.629$ ($p = 8.88 \times 10^{-5}$) for k_D versus age, $r = 0.492$ ($p = 0.0037$) for k_P versus age, and $r = 0.618$ ($p = 1.27 \times 10^{-4}$) for k_{PD} versus age. The robust correlation

for k_D against age serves as a strong validation of our methodology in reproducing the established Yarkovsky chronometer. More importantly, the statistically significant correlations found for k_P and k_{PD} against age represent novel empirical evidence, demonstrating that an asteroid's spin period is a measurable and significant factor in its long-term orbital evolution within a family. While the correlation for k_P was weaker than for k_D and k_{PD}, this is consistent with the greater physical complexity of spin-dependent Yarkovsky effects, which are modulated by factors such as obliquity and the YORP effect.

From these findings, we have learned that the Yarkovsky effect's influence on asteroid orbits is not only size-dependent but also demonstrably spin-dependent over cosmic timescales. This study empirically confirms the crucial role of spin in the long-term orbital evolution of asteroid families, validating theoretical predictions and establishing a novel framework for analyzing spin-orbit coupling. The derived coefficients offer new physically-grounded chronometers that can be used to refine asteroid family ages, providing independent constraints on their formation times. Furthermore, the framework provides a valuable tool for constraining thermophysical models of asteroids, as the empirically measured drift rates are directly related to properties like thermal inertia and surface conductivity. Despite limitations stemming from data sparsity, inherent measurement uncertainties, and physical model simplifications (such as assuming linear relationships or neglecting obliquity and YORP evolution), this work represents a significant step forward in our empirical understanding of asteroid dynamics and the forces shaping the Solar System's minor body populations. Future work can aim to incorporate more sophisticated physical models and account for observational biases to further refine these empirical relationships.